432 *Biochemistry* **2010,** *49,* 432–442
DOI: 10.1021/bi901583n

BIOCHEMISTRY
including biophysical chemistry & molecular biology
Article

An Unusual Pattern of CytR and CRP Binding Energetics at *Escherichia coli cddP* Suggests a Unique Blend of Class I and Class II Mediated Activation†

Allison K. Holt and Donald F. Senear*

Department of Molecular Biology and Biochemistry, University of California, Irvine, California 92697

Received September 9, 2009; Revised Manuscript Received November 4, 2009

ABSTRACT: Two transcription factors, CRP and CytR, mediate positive and negative control of nine cistrons involved in nucleoside catabolism and recycling in *Escherichia coli*. The ability of multiple transcription factors to combine in different ways to confer differential gene regulation is of significant interest in both prokaryotic and eukaryotic gene regulation. Analysis of cooperative interactions between CytR and CRP at the *deoP2* and *udpP* promoters has implicated the importance of promoter architecture in controlling repression and induction. These studies have also identified competition between CytR and CRP as an additional contributor to differential regulation. The pattern and energetics of CytR and CRP interactions at the *cdd* promoter, the most strongly activated of the CytR-regulated promoters, have been delineated using DNase I footprinting. Surprisingly, CRP has greater affinity for the promoter proximal site at *cddP*, CRP1, than for the distal site, CRP2, in contrast to promoters studied previously. This difference is a major contributor to unusually high CRP-mediated activation of *cddP*. Additionally, while cytidine binding to CytR nearly eliminates the pairwise interactions between CytR and CRP bound at CRP1, it has little effect on pairwise cooperativity between CytR and CRP bound at CRP2 or as a consequence on the overall cooperativity of the three-protein complex in which CRP is bound to both sites. The effect of cytidine binding on cooperativity differs between the three promoters studied thus far. We propose that the different patterns of interaction reflect the spacing between CytR half-sites and the location of the CytR operator in relation to the two CRP sites.

Combinatorial control is a ubiquitous feature of transcriptional regulation in both prokaryotic and eukaryotic organisms. Typically, multiple regulatory proteins (factors) that bind to specific DNA sites (regulatory elements) are used to control the transcription of individual genes. These multiprotein complexes direct the recruitment and activation of RNA polymerase. The arrangement of regulatory elements along the DNA generates a scaffold that can either constrain or facilitate interactions among the transcription factors and between the transcription factors and the polymerase. The resulting hierarchy of effects has the capacity for regulation that is nearly continuously adaptable to developmental, physiological, or environmental conditions. In addition, individual transcription factors typically contribute to the regulation of multiple promoters, thus providing a mechanism to coordinate the regulation of multiple genes; modulation of the activity of individual factors can be used to trigger broad patterns of gene expression.

The *Escherichia coli* CytR[1] regulon presents a simple paradigm for coordinate control of gene expression. It comprises nine operons that encode genes for nucleoside transport and catabolism (*1*, *2*). Control of these operons is mediated by two, DNA-binding transcription factors: the regulon-specific, cytidine repressor protein (CytR), and the cAMP receptor protein (CRP), a widely used activator of catabolic genes. With only these two transcription factors, the CytR regulon represents the simplest possible model of combinatorial gene regulation. Yet this simple system delivers differential control of the individual operons. The regulatory variability is remarkable. For example, CRP-mediated activation ranges from a robust approximately 30-fold for *deoP2* (*2*) to several hundred-fold for *cddP* (*2*, *3*). CytR-mediated repression is similarly quite variable, ranging from only 6−12-fold at *deoP2* (*2*, *4*, *5*) to 50−100-fold at *cddP* (*2*, *3*, *6*). It is of considerable interest to understand how promoter architectures that involve so few components elicit such varied responses.

The CytR regulon presents an attractive model system at two levels. First, CytR is member of the LacI/GalR family of transcription regulators. Homologues are found in all bacteria evaluated, with more than 1000 members known (*7*) and 16 paralogues identified in *E. coli* (*8*). The family members typically sense environmental or metabolic conditions by binding an effector ligand to a regulatory domain, an interaction that is then coupled to the DNA-binding affinity of a distinct DNA-binding domain. CRP activates transcription of about 200 genes in *E. coli* (*9*) in response to the carbon source available. As one of the most thoroughly studied gene activators, CRP serves as a model for mechanisms of transcriptional activation (*10*). Opposing activation and repression, mediated by CRP and a LacI family member, respectively, is one of the most common ways in which transcription of catabolic genes is regulated in bacteria to meet the cell's metabolic needs. In addition to this, the differential

†The research was supported in part by Grants MCB-0215769 and MCB-0719373 from the National Science Foundation (NSF). The contents of this publication are solely the responsibility of the authors and do not necessarily represent the official views of the NSF.

*To whom correspondence should be addressed. Phone: (949) 824-8014. Fax: (949) 824-8551. E-mail: dfsenear@uci.edu.

[1]Abbreviations: bistris, 2-[bis(2-hydroxyethyl)amino]-2-(hydroxymethyl)-propane-1,3-diol; CRP, *Escherichia coli* cyclic AMP receptor protein; CytR, *Escherichia coli* cytidine repressor protein; DNase I, deoxyribonuclease I; RNAP, bacterial RNA polymerase, Tris, tris(hydroxymethyl)aminomethane; EDTA, ethylenediaminetetraacetic acid.

 Published on Web 12/10/2009

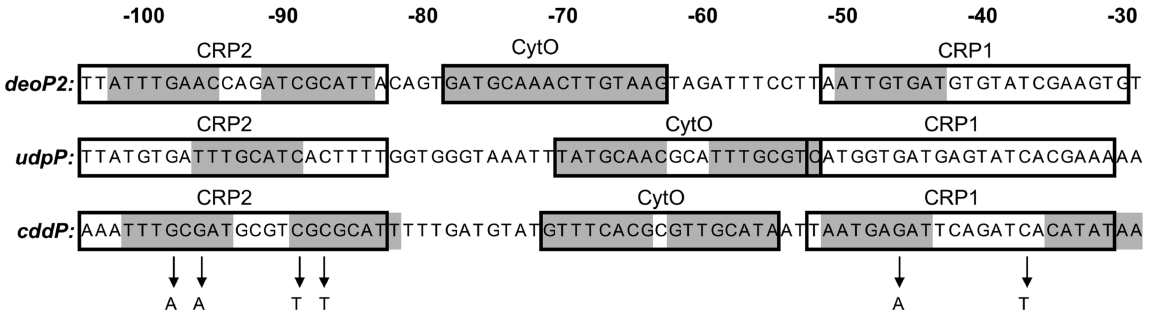

FIGURE 1: Upstream regulatory sequences of *deoP2*, *udpP*, *nupGP*, and *cddP*. CRP sites (*CRP1* and *CRP2*) and the CytR operator (*CytO*) are delineated by open boxes; CytR recognition motifs are shaded. The transition of two G/C base pairs in CRP1 to A/T eliminates sequence-specific binding by CRP to CRP1 to yield a promoter we designate CRP1^{-}. Similarly, transition of the corresponding base pairs in CRP2 generates CRP2^{-}. Two additional mutations were introduced to eliminate the possibility of sequence-specific CRP binding in an altered register shifted two base pairs downstream.

regulation exhibited by the CytR regulon presents a useful paradigm for more widespread mechanisms of coordinate regulation in both prokaryotes and eukaryotes.

The potential for widely variable regulatory properties among CytR-regulated promoters resides both in their unusual utilization of CRP and in properties that are unique to CytR. Four CytR-regulated promoters (*cddP*, *deoP2*, *nupG*, *udpP*) feature tandem CRP operators flanking a central CytR operator (CytO). These have nearly identical architectures as shown in Figure 1. Each contains both a proximal CRP site (CRP1) that overlaps the −35-promoter element and a distal site (CRP2) located at −91 to −93 bp. These function synergistically. CRP utilizes a class I activation mechanism when bound to either CRP1 or distal CRP2 site (*11*−*16*). A class I mechanism refers to interactions between CRP and the C-terminal domain of the α-subunit (αCTD) of RNAP that serve to recruit RNAP to the promoter. However, CRP bound to CRP1 (but not CRP2) also utilizes a class II mechanism. This refers to interactions between CRP and the N-terminal domain of the α-subunit (αNTD) of the polymerase that increase the rate of open complex formation (*14*, *15*, *17*). Promoters that feature both class I and class II mechanisms are referred to as class III promoters.

A critical component of the regulation is that CytR and CRP bind DNA cooperatively, meaning that CRP binding to CRP1 and CRP2 enhanced the affinity of CytR for CytO and vice versa (*18*, *19*). As a result of this cooperativity CytR is recruited to CytO when CRP binds to the flanking sites, CRP1 and CRP2, to yield a three-protein, DNA-bound complex, CRP-CytR-CRP. Even with its DNA-binding domain deleted, CytR will associate to form a protein bridge between CRP dimers bound to CRP1 and to CRP2, thus indicating that direct interaction between the DNA-bound proteins is the mechanism for the cooperativity (*20*). In the three-protein complex, CytR competes with RNAP both for binding to the DNA and also for interaction with CRP. The significance of CytR-CRP cooperativity to this competition is underscored by the fact that binding of cytidine (the inducer ligand) to CytR is coupled to CytR-CRP cooperativity (*19*, *21*), a feature that is unique among LacI family repressors. Unlike all other *E. coli* paralogues, for which binding of the regulatory ligand, whether inducer or corepressor, is linked to DNA-binding affinity, the intrinsic affinity of CytR for CytO is unaffected by cytidine binding to CytR (*19*).

One approach to understanding the molecular mechanism(s) of differential regulation in the CytR regulon has been to compare the cooperative energetics of protein−DNA and protein−protein interactions at the different promoters. The energetics governs the distributions of ligation states of the various promoters. We anticipate that varying distributions will correlate to differing regulatory properties. We have reported previously on two promoters, *deoP2* and *udpP* (*19*, *22*, *23*). The most striking difference we find is a very different pattern of cytidine-mediated effects on CytR-CRP cooperativity. Whereas at *deoP2* cytidine binding to CytR essentially eliminates cooperativity in the three-protein complex, at *udpP* it serves to eliminate cooperativity only between CytR and CRP bound to CRP1. Combined with differences in intrinsic binding affinities of the individual transcription factors, this appears to underlie different extents of cytidine-mediated induction.

We now report the energetics of CytR-CRP-DNA interaction at the cytidine deaminase promoter (*cddP*), the CytR-regulated promoter with the highest fold activation and highest fold repression. Do differences in underlying protein−protein and protein−DNA interaction energetics explain the unusually high extents of activation, repression, and induction of *cddP*? Quantitative DNase I footprint titration was used to obtain the individual site isotherms for binding of each regulatory protein to each site in *cddP*. Analysis of these isotherms allowed us to obtain the individual site loading free energy changes for each site of interaction, from which we deduced the presence of both cooperative and competitive binding interactions. Global analysis of these data according to a model that accounts for the individual and cooperative interactions yielded the Gibbs free energy change for each.

This analysis yielded two striking results. First, the relative affinities of CRP for binding to CRP1 and to CRP2 are reversed as compared to other CytR-regulated promoters; at *cddP*, the CRP1 site is the higher affinity site. This feature accounts for the unusual effectiveness of CRP to activate expression of cytidine deaminase. Second, cytidine binding to CytR generates a different pattern of effects on CytR-CRP cooperativity from what is observed for either *deoP2* or *udpP* (*19*, *22*). At *cddP*, cooperativity between CytR and CRP bound to CRP1 is largely retained, while cooperativity between CytR and CRP bound to CRP2 is largely eliminated. This pattern of cooperative effects adds to the diversity of cytidine-mediated allosteric effects in CytR and provides a ready explanation for the different extents of induction of gene expression as are observed. However, we can only speculate as to the nature of the structural mechanisms that underlie the different effects on CytR-CRP binding cooperativity.

MATERIALS AND METHODS

Reagents and Enzymes. Crystalline cAMP (>99% pure as free base) and cytidine (>99% pure as free acid) were purchased

from Boehringer Mannheim and Sigma, respectively. Stock solutions were prepared, and purity was assessed and concentration determined all as described previously (*19*). Bovine pancreas DNase I (code DPRF from Worthington) was stored in a buffer containing 50 mM Tris (pH 7.20 ± 0.01), 10 mM $MgCl_2$, 1 mM $CaCl_2$, 1 mM DTT, and 50% (w/v) glycerol. [α-^{32}P]Deoxyribonucleoside triphosphates (3000 Ci/mmol) were obtained from PerkinElmer; unlabeled deoxyribonucleoside triphosphates were purchased from Nitrogen. All other buffer components were of electrophoresis grade or equivalent if available or of reagent grade otherwise.

CRP and CytR Purification. Overexpression of CRP from plasmid pPLcCRP1 (*24*) in *E. coli* strain K12 and purification to at least 98% homogeneity have been described previously (*19*). CRP concentration was estimated based on a calculated extinction coefficient, ε = 18400 M^{-1} cm^{-1} at 280 nm. Under the reaction conditions used, the fraction of CRP in its active, site-specific DNA-binding form in which cytidine is bound to one but not both subunits, denoted as CRP(cAMP$_1$), is 0.64 ± 0.2 (*19*). CytR was expressed in *E. coli* strain BL21(DE3) and purified as described previously (*21*). CytR prepared in this manner is at least 95% pure as determined by electrophoresis on SDS−polyacrylamide gels in a reducing environment. The concentration of CytR was estimated based on an extinction coefficient at 276 nm of 9460 (±250) M^{-1} cm^{-1} (*25*).

Promoter DNA Preparation. The *cdd* promoter containing DNA was obtained from *E. coli* strain K12 genomic DNA by PCR. Primers were designed to amplify the 297 bp region from −153 to +144 relative to the *cdd* transcription start. The purified PCR product was cloned into the Srf1 site of Stratagene PCR-Script Amp SK(+) plasmid to generate plasmid pMRcdd. Promoter-containing DNA fragments (299 bp), generated by restriction digestion with *Sma*I (at a site created by ligation of the PCR product into the vector Srf I site) and *Bam*HI, were purified by agarose gel electrophoresis. The *Bam*HI site was used for ^{32}P labeling using the Klenow fill-in reaction (*26*).

Mutant promoters were designed to eliminate site-specific CRP binding to either CRP1 (CRP1$^-$) or CRP2 (CRP2$^-$). The transition of two G/C base pairs to A/T is sufficient to eliminate site-specific CRP binding. We refer to these as reduced-valence promoters. We also mutated a putative overlapping CRP2 site shifted two base pairs downstream (*6*) at its corresponding G/C base pairs. Base pair substitutions were generated using the QuikChange site-directed mutagenesis kit from Stratagene and the sequences (Figure 1) confirmed by dideoxy sequencing.

Individual Site Binding Experiments. Quantitative DNase footprint titrations were conducted as described previously (*19*, *22*). The experiments with CRP contained 150 μM cAMP, a concentration that maximizes the fraction of CRP in its active form (0.64 ± 0.2) under these buffer conditions (*19*). The binding buffer is 10 mM bistris, 100 mM NaCl, 0.5 mM each $CaCl_2$ and $MgCl_2$, 1.0 mM NaN_3, 50 g/L ovalbumin, and 1 g/L CT-DNA. Binding reactions (250 μL) were incubated for at least 30 min in a constant temperature water bath at 20.0 ± 0.05 °C prior to addition of 6−12 ng of DNase I in a 5 μL volume. DNase I reaction was quenched after 12.0 min by addition of 50 μL of 50 mM NH_4EDTA and rapid mixing, followed immediately by addition of stop solution (90% ethanol, 1 M ammonium acetate, and 0.014% polymerized linear acrylamide) (*19*) at −80 °C. The DNA was precipitated, and the pellets were washed in 80% ethanol prior to being dissolved in 7 μL of gel loading solution containing 90% USB stop solution, 5% 10× TBE, and 5% ddH_2O. DNA was separated by electrophoresis at 50 W for approximately 1.5 h in 0.4 mm, 4% gels (Long Ranger single pack from Cambrex; part no. 50694). Dried gels were imaged by exposing a Molecular Dynamics (now GE) storage phosphor screen for approximately 3 days. Images were scanned at 176 μM resolution using a Molecular Dynamics PhosphorImager 435 SI.

The footprints were first analyzed using the program SAFA (*27*) to delineate contiguous groups (or blocks) of bands that are protected from DNase I cleavage resulting from transcription factor binding to the individual operator sites. A ^{32}P-labeled 100 base pair DNA ladder was used as a reference to aid in identifying the promoter locations corresponding to these blocks. Subsequently, each block was analyzed using Image Quant (v.5.2) to obtain the individual-site fractional protection, as described previously (*28*, *29*). These data were first analyzed separately according to

$$P_{\mathrm{obs},i} = P_{\mathrm{o},i} + (P_{\mathrm{max},i} - P_{\mathrm{o},i})\left(\frac{e^{(-\Delta G_{\mathrm{app},i}/RT) + \ln[\mathrm{L}]}}{1 + e^{(-\Delta G_{\mathrm{app},i}/RT) + \ln[\mathrm{L}]}}\right) \quad (1)$$

where P_{obs} is the fractional protection observed for binding site i at the free protein ligand concentration [L], $\Delta G_{\mathrm{app},i}$ is the Gibbs free energy change that corresponds to the apparent association equilibrium constant for binding to site i ($\Delta G = -RT \ln K_a$), and P_o and P_{max} are the baseline and maximum fractional protection attained at site i (*30*). $\Delta G_{\mathrm{app},i}$ provides a reasonable estimate of the individual site loading free energy change, $\Delta G_{\mathrm{Load},i}$ (*31*), and its confidence limits (*23*). This model-independent quantity reflects all interactions, including not only intrinsic binding but also cooperative and competitive interactions resulting from interactions at other sites (*23*, *31*).

Subsequently, global analysis of the individual site CRP and CytR binding data was conducted according to the model that is defined by the promoter configurations described in Table 3. By accounting for all of the data in a global analysis, we are able to determine accurately the intrinsic affinities for each transcription factor−DNA interaction and the contributions from cooperativity, competition, and induction for each molecular configuration of *cddP*. The relative probability, f_s, of any single promoter configuration is given by

$$f_s = \frac{e^{((-\Delta G_s/RT) + i\ln[\mathrm{CRP(cAMP)_1}] + j\ln[\mathrm{CytR}])}}{\sum_{sij} e^{((-\Delta G_s/RT) + i\ln[\mathrm{CRP(cAMP)_1}] + j\ln[\mathrm{CytR}])}} \quad (2)$$

ΔG_s is the sum of all free energy contributions for a given configuration, s (Table 3); i and j are the stoichiometries of bound CRP(cAMP)$_1$ and CytR in configuration s, respectively. The equation for binding of a protein, CRP(cAMP)$_1$ or CytR, to an individual site is obtained by summing f_s over all configurations in which that protein is bound to that individual site. To obtain binding equations for the two reduced-valence operators, CRP1$^-$ and CRP2$^-$, configurations in which CRP(cAMP)$_1$ is bound to a mutated site were excluded from the summations.

Global analysis was performed as described previously (*19*, *32*). The nonlinear least-squares estimation was performed using Igor Pro 5.05. Variances from the individual analyses of each binding curve using eq 1 were used to calculate normalized weights. Parameter confidence limits reported by Igor Pro are computed from the curvature at the minimum assuming a linear fitting model. However, the model described in Table 3 is

nonlinear and features strongly correlated parameters. Therefore, to estimate parameter confidence limits for the eight ΔG's of this model, each of these parameters was varied systematically while repeating the global analysis to estimate the remaining parameters (both ΔG's and $P_{o,i}/P_{max,i}$). The ratio of the variance obtained for each such fit to the variance at the global minimum was calculated. Ratios of variances were also separately calculated considering the data obtained for each binding site and set of effectors, e.g., for binding of CytR to CytO of the wild-type promoter in the presence of CRP and cytidine. The confidence limits reported correspond to the more restrictive of two criteria: (i) a ratio of variances for the global analysis corresponding to F_{stat} at the 65% confidence interval or (ii) a ratio of variances for any binding site and set of effectors corresponding to F_{stat} at the 95% confidence interval.

RESULTS

Analysis of Molecular Interactions at cddP. Our previous analysis of the binding of CytR and CRP to the *deoP2* and *udp* promoters has highlighted unique aspects of these interactions that appear to be related to differential regulation of the CytR-regulated promoters. One surprise uncovered by our analysis of *deoP2* is that, in addition to its site-specific binding to CytO, CytR also binds with weak specificity to satellite sites and that this binding competes with CRP for binding to both CRP1 and CRP2 (*19*). A second surprise uncovered by our analysis of *udpP* is that the inducer cytidine does not eliminate all CytR-CRP cooperativity, as it does at *deoP2*, but instead eliminates only the pairwise interaction between CRP bound to CRP1 and CytR bound to CytO (*22*). On the basis of these findings, we sought to understand the pattern of molecular interactions at *cddP* because this promoter features much higher levels of activation and repression. Can this difference be readily explained by differences in the underlying molecular interactions?

Footprint Titration of CytR Binding. CytR binding to the *cddP* DNA fragment was analyzed by DNase I footprint titration. CytR binding protects an extended region of the promoter, from about bp to −120 to +10, measured relative to the transcription start site (Figure 2A). This extended region of protection includes CytO and both flanking CRP sites. In addition, there is a clear hypersensitive region just distal to the CRP2 site, at approximately −125 bp. On the basis of previous analysis of CytR binding to both *deoP2* and *udpP*, we anticipated that the extended protection pattern reflects CytR binding to multiple distinct sites in this region.

As a first step in the analysis of this protection, two footprints were analyzed on an band-by-band basis using the software program SAFA (Semi-Automated Footprint Analysis) (*27*) to define the regions of protection corresponding to different sites of CytR binding. SAFA uses automated band detection to quantitate separately every band within a user-selected region. The concentration dependence of each identifiable band, both protected and hypersensitive, was fitted separately to the simple binding model given in eq 1 to obtain ΔG_{app} (with confidence intervals). Contiguous groups of bands that yielded indistinguishable ΔG_{app} were interpreted to reflect the same local binding event.

This analysis identified four distinct regions of protection (Figure 2A). The highest affinity binding corresponds to the location of the CytR operator (CytO). Additional distinct regions of protection that overlap CRP1 and CRP2 mimic the satellite

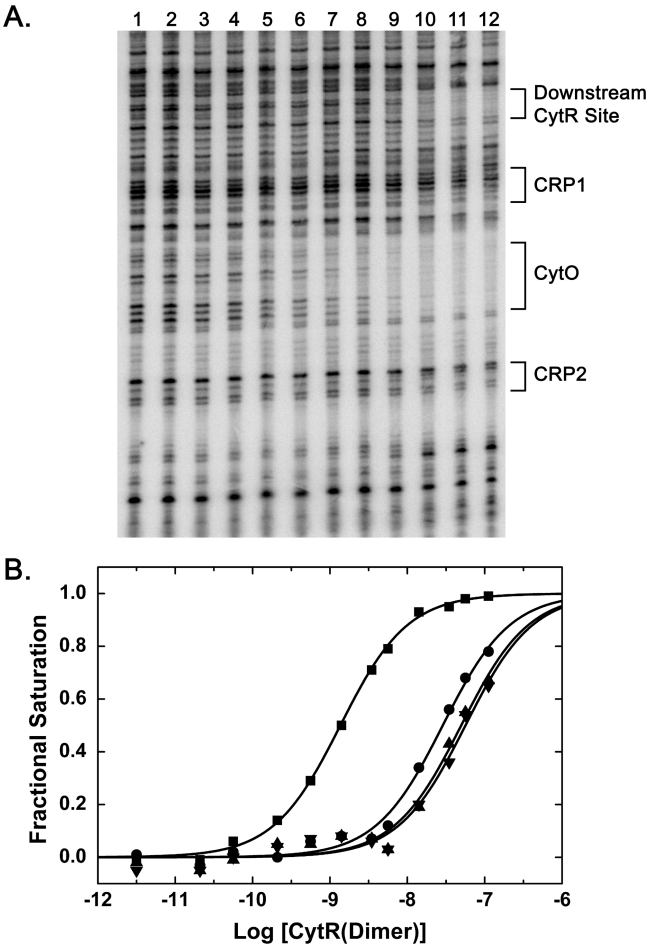

FIGURE 2: CytR binding to the *cddP* regulatory region. (A) DNase I footprint titration conducted under standard conditions shows increasing protection as a function of CytR concentration in lanes 1−12. Lane 1 shows the cleavage pattern in the absence of CytR. Protected regions corresponding to operator sites *CRP1*, *CytO*, and *CRP2* and to an additional promoter-proximal site (see text) are labeled at right. These indicate the blocks of bands used for analysis of CytR binding to these sites. (B) Individual site curves for CytR binding to the *cddP* obtained by analysis of the data shown in (A). Fractional saturation of CytO (■), CRP1 (▲), CRP2 (▼), and the downstream site (●) is plotted as a function of log CytR dimer concentration. An arbitrarily small value was chosen to plot the value from lane 1. Solid curves represent the individual analysis of the protection data for each site according to eq 1; these yield apparent individual site loading free energy changes equal to -11.9 ± 0.1 kcal/mol (CytO), -9.8 ± 0.4 kcal/mol (CRP1), -9.7 ± 0.5 kcal/mol (CRP2), and -10.1 ± 0.2 kcal/mol (downstream CytR site).

CytR sites identified in both *deoP2* and *udpP* (*19*, *22*). An additional region of protection suggests a CytR site located just downstream from the transcription start site.

Contiguous groups or "blocks" of bands corresponding to each of these sites were analyzed using the program ImageQuant as described previously (*19*). The footprint data shown in Figure 2A were analyzed using eq 1 (Figure 2B) to obtain the loading free energy changes for each of the individual site interactions. As we have shown previously (*19*, *22*), there are no cooperative interactions between CytR dimers binding to distinct locations. Therefore, each loading free energy change so obtained is equivalent to the intrinsic free energy change for CytR binding to the local site. Analysis of the experiment represented in Figure 2 yielded intrinsic free energy changes of -11.9 ± 0.1 kcal/mol for CytR binding to CytO and -9.8 ± -0.4

Table 1: Loading Free Energy Changes for Binding of CRP and CytR to the *cdd* Regulatory Region[a]

				operator site				
cdd valence	titrant	effector[b]	no. of expts[c]	CRP2	CytR at CRP2	CytO	CRP1	CytR at CRP1
wild type CRP1$^-$ CRP2$^-$	CRP	none	7	-12.4 ± 0.4			-13.8 ± 0.3	
wild type CRP1$^-$ CRP2$^-$	CytR	none	10		-9.6 ± 0.5	-11.5 ± 0.2		-9.7 ± 0.2
wild type	CRP	CytR	2	-12.8 ± 0.1			-13.7 ± 0.2	
CRP1$^-$	CRP	CytR	2	-13.3 ± 0.1				
CRP2$^-$	CRP	CytR	3				-14.1 ± 0.1	
wild type	CytR	CRP	4			-13.2 ± 0.3		
CRP1$^-$	CytR	CRP	2			-13.4 ± 0.4		
CRP2$^-$	CytR	CRP	3			-13.3 ± 0.3		
wild type	CRP	CytR, cytidine	3	-12.2 ± 0.3			-14.3 ± 0.3	
CRP1$^-$	CRP	CytR, cytidine	2	-12.1 ± 0.0				
CRP2$^-$	CRP	CytR, cytidine	2				-14.5 ± 0.03	
wild type	CytR	CRP, cytidine	5			-12.9 ± 0.4		
CRP1$^-$	CytR	CRP, cytidine	2			-12.3 ± 0.2		
CRP2$^-$	CytR	CRP, cytidine	2			-12.8 ± 0.1		

[a]Free energy changes for saturation of *cdd* operators with either CRP(cAMP)$_1$ or CytR in the presence or absence of effector ligands are as indicated. Values of ΔG_1 (in kcal/mol) were obtained by separate analysis of individual site binding curves as described in the text. [b]Effector concentrations: CRP, 0.1 μM (total dimer); cAMP, 150 μM; CytR, 0.1 μM (dimer); cytidine, 2 mM. [c]$\Delta G_{\mathrm{Load},i}$ values are shown as the means of multiple determinations (±SD). The number of separate experiments represented in the means reported is indicated.

and -9.7 ± -0.5 kcal/mol for binding to the sites overlapping CRP1 and CRP2, respectively.

In addition to the wild-type *cddP*, experiments were also conducted using reduced-valence promoters, CRP1$^-$ and CRP2$^-$. Consistent with our previous results (*19*, *22*), introduction of these base pair changes had no effect on CytR binding to nonmutated sites. Table 1 summarizes results obtained from all ten experiments conducted on wild type and CRP1$^-$ and CRP2$^-$ promoters. These results indicate higher affinity for CytR binding to CytO at *cddP* than for binding to CytO of either *udpP* (about 3-fold) or *deoP2* (about 7-fold). The CytR binding affinity for the satellite sites overlapping CRP1 and CRP2 is also 3−5-fold higher than for the corresponding sites at *deoP2*, though similar to the CRP2 site at *udpP*.

The fourth distinct region of protection was also analyzed. The band resolution near the top of the gel is insufficient to define the precise location of this CytR binding site. However, we note a pair of sequences with close matches to the CytR half-site consensus sequence located just downstream from the transcription start site. These might constitute a specific CytR binding site centered at +13 bp, albeit with unusual spacing of five base pairs between recognition half-sites. Analysis of this protected region as shown in Figure 2B resulted in an intrinsic free energy change for binding of -10.1 ± 0.2 kcal/mol.

Footprint Titration of CRP Binding. CRP binding to *cddP* was also analyzed using DNase I footprint titration. Titration experiments were conducted using both wild-type *cddP* and also the CRP1$^-$ and CRP2$^-$ promoters. For both reduced-valence mutants, the free energy change for binding to the nonmutated site was indistinguishable from the value obtained for binding to the wild-type *cddP*. We conclude on this basis, first, that the particular base pair substitutions in the mutated sites have no effect on binding to the nonmutated sites and, second, that CRP binding is noncooperative. Both conclusions were drawn previously from our analysis of *deopP2* and *udpP* (*19*, *22*). Table 1 summarizes the combined results of experiments conducted on wild type and CRP1$^-$ and CRP2$^-$ promoters. The CRP affinity for CRP1 of *cddP* is about 10-fold higher than for CRP2. This is the opposite order of affinity from that observed for other CytR-regulated operators. It confirms a semiquantitative result reported previously (*3*).

Table 2: Apparent Cooperativity[a] As Assessed by Differences in Individual Site Loading Free Energy Changes Described in Table 1

titrant	$\Delta G_{\mathrm{app}}123$	$\Delta G13_{\mathrm{app}}$	$\Delta G23_{\mathrm{app}}$
CytR	-1.7 ± 0.4	-1.8 ± 0.4	-1.9 ± 0.4
CRP	-0.3 ± 0.4	-0.3 ± 0.4	-0.9 ± 0.4

[a]$\Delta G_{\mathrm{app},ij(k)}$ values calculated as model-independent values are the differences in ΔG_1 values given in Table 1. These apparent free energy changes are associated with pairwise and three-way cooperativity as defined by the model in Table 2. Confidence levels are estimated by error propagation.

Analysis of Cooperative and Competitive Binding of CRP and CytR. We evaluated the cooperative interactions and competition between CytR and CRP as described previously (*19*, *22*). This analysis requires two types of binding experiments. First, binding by each protein alone to wild type and reduced-valence promoters is analyzed, as described just above. Second, binding of each protein (CytR and CRP) to each promoter is analyzed in the presence of a fixed and saturating concentration of the other protein (CRP and CytR, respectively). As a practical limit to saturating concentration, 0.1 μM dimer was used for both CRP and CytR. This concentration of CytR yields 98% saturation of CytO and about 60% saturation of each of the CytR sites that overlap CRP1 and CRP2. The concentration of cAMP used in these experiments (150 μM) maximizes the fraction of CRP dimer in the active form as CRP(cAMP)$_1$ (0.64 ± 0.02) (*19*). At a concentration of 64 nM CRP(cAMP)$_1$, the fractional saturation exceeds 99% for both CRP1 and CRP2.

The individual-site loading free energy changes ($\Delta G_{\mathrm{Load},i}$) obtained from these experiments are summarized in Table 1. These loading free energy changes include both the intrinsic free energy change for protein binding to the local site and contributions from binding to all coupled sites, either cooperatively interacting or competing. For a system in which only intrinsic binding and cooperativity contribute, the difference between $\Delta G_{\mathrm{Load},i}$'s obtained for binding of either protein (CytR or CRP) in the presence versus absence of the other yields the cooperativity. Considering the values listed in Table 1 for CytR binding to CytO

Table 3: Configurations and Free Energy States for CRP and CytR Binding to the *cdd* Promoter

	binding sites[a]						
	CRP2	CytR at CRP2	CytO	CRP1	CytR at CRP1	free energy contributions[b]	free energy state
1	O	O	O	O	O	reference state	$\Delta G_{s,1}$
2	O	O	O	CRP	O	ΔG_1	$\Delta G_{s,2}$
3	CRP	O	O	O	O	ΔG_2	$\Delta G_{s,3}$
4	O	O	CytR	O	O	ΔG_3	$\Delta G_{s,4}$
5	O	O	O	O	CytR	ΔG_4	$\Delta G_{s,5}$
6	O	CytR	O	O	O	ΔG_5	$\Delta G_{s,6}$
7	CRP	O	O	CRP	O	$\Delta G_1 + \Delta G_2$	$\Delta G_{s,7}$
8	O	O	CytR	CRP	O	$\Delta G_1 + \Delta G_3 + \Delta G_{13}$	$\Delta G_{s,8}$
9	O	CytR	O	CRP	O	$\Delta G_1 + \Delta G_5$	$\Delta G_{s,9}$
10	CRP	O	CytR	O	O	$\Delta G_2 + \Delta G_3 + \Delta G_{23}$	$\Delta G_{s,10}$
11	CRP	O	O	O	CytR	$\Delta G_2 + \Delta G_4$	$\Delta G_{s,11}$
12	O	O	CytR	O	CytR	$\Delta G_3 + \Delta G_4$	$\Delta G_{s,12}$
13	O	CytR	CytR	O	O	$\Delta G_3 + \Delta G_5$	$\Delta G_{s,13}$
14	O	CytR	O	O	CytR	$\Delta G_4 + \Delta G_5$	$\Delta G_{s,14}$
15	CRP	O	CytR	CRP	O	$\Delta G_1 + \Delta G_2 + \Delta G_3 + \Delta G_{123}$	$\Delta G_{s,15}$
16	CRP	O	CytR	O	CytR	$\Delta G_2 + \Delta G_3 + \Delta G_4 + \Delta G_{23}$	$\Delta G_{s,16}$
17	O	CytR	CytR	O	CytR	$\Delta G_3 + \Delta G_4 + \Delta G_5$	$\Delta G_{s,17}$
18	O	CytR	CytR	CRP	O	$\Delta G_1 + \Delta G_3 + \Delta G_5 + \Delta G_{13}$	$\Delta G_{s,18}$

[a]Binding sites are listed in columns 2−6 corresponding to the order, from promoter distal to promoter proximal, on the DNA. Each table row, 1−18, describes a particular configuration of protein-bound (filled) and empty sites. CRP and CytR designated filled sites according to the transcription factor bound; O designates empty sites. [b]The total Gibbs free energy of each configuration relative to the unliganded reference state is given as a sum of contributions from five free energy changes for intrinsic binding of CRP and CytR and three free energy changes for cooperative interaction between liganded sites. Subscripts denote the liganded sites: 1, CRP1; 2, CRP2; 3, CytO; 4, CytR site(s) that overlap(s) and occlude(s) CRP1; 5, CytR site(s) that overlap(s) and occlude(s) CRP2.

of the wild-type *cddP*, this analysis suggests a total cooperative free energy change of −1.7 kcal/mol.

In principle, the same value should be obtained by summing the $\Delta(\Delta G_{\mathrm{Load},i})$ values for CRP binding to CRP1 and to CRP2 in the presence versus absence of saturating CytR. The results of this simple analysis (Table 2) clearly contradict this expectation. The reason for this is that competition between CRP for binding to CRP1 and CRP2 and CytR for binding to satellite sites that occlude CRP1 and CRP2 complicates this simple analysis. Competition contributes differently to ΔG_1 and ΔG_2 for CRP binding to CRP1 and to CRP2 in the presence of fixed CytR concentration than it does to ΔG_3 for CytR binding to CytO in the presence of fixed CRP concentration. This has the effect that the apparent cooperativity evaluated from CRP titrations in this manner is almost negligible, an effect noted also and evaluated extensively in our analysis of *deoP2* and *udpP* (*19*, *22*). As a consequence of these effects, dissection of the energetics to obtain the intrinsic binding and cooperative free energy changes requires global analysis of all of the titration experiments according to the appropriate molecular model that accounts for all contributing configurations of the promoter.

Global Analysis. The molecular model defined by the promoter configurations listed in Table 3 accounts for CRP binding to CRP1 and to CRP2 and for CytR binding to CytO, with both pairwise and three-way CytR-CRP cooperativity. In this model, binding of CytR at the sites overlapping CRP1 and CRP2 and of CRP binding to CRP1 and CRP2 is mutually exclusive. The model neither implies nor requires specification of the specific location of the occluding CytR sites. Although CytR binds to an additional site located just downstream from the transcription start site as noted above, there is no interaction between CytR binding to this site and CytR/CRP binding to CRP2, CytO, and CRP1. Since binding to this site is fully described by the intrinsic binding free energy change alone, this site is not included in the model presented in Table 3. In addition, we note that the mutations used to create the reduced-valence CRP1$^-$ and CRP2$^-$ promoters resulted in a 2−3-fold increase in CytR binding affinity for the competing sites in both cases. However, because CRP does not bind to the mutated sites, hence there is no competition, this effect is not coupled to the interactions with the remaining operator sites and so need not be included in the model.

Figure 3 shows the binding curves that result from the global analysis of 48 experiments represented in Table 1 according to this model. The χ^2 value obtained in this weighted fit is 2.3. This is higher than χ^2 values obtained from the analogous global analyses of *deoP2* and *udpP*. However, it is consistent with the reproducibility between repeated footprint titration experiments. So, for example, when all of the experiments represented in either of the first two lines of Table 1 (i.e., only intrinsic binding to each of the operator sites) were analyzed globally, χ^2 values obtained for each of the individual sites ranged from close to 1 to almost 4. The curves obtained from the complete global analysis fit the titration data well for each operator site and for each protein and combination of effectors, as evidenced by residuals that are nearly randomly distributed in every case (Figure 3) from which we conclude that the model presented in Table 3 is an adequate depiction of the molecular interactions in this system.

This analysis did not fit the protection data for CytR binding to the satellite sites that overlap CRP1 and CRP2. Relatively weak binding affinity and limited range of CytR concentration led to poorly defined protection upper end points in most titrations of these sites. When these data were included in the analysis, these end points were unbounded. However, the values obtained for ΔG_4 and ΔG_5, -9.6 ± 0.7 kcal/mol and −9.6 (+0.5, −0.6) kcal/mol, respectively, are indistinguishable from $\Delta G_{\mathrm{Load},i}$ obtained for these sites (Table 1). In addition, when these data were not included in the analysis but ΔG_4 and ΔG_5 were fit as adjustable parameters, these same values were obtained. Thus, defining these sites thermodynamically, by their effect on the

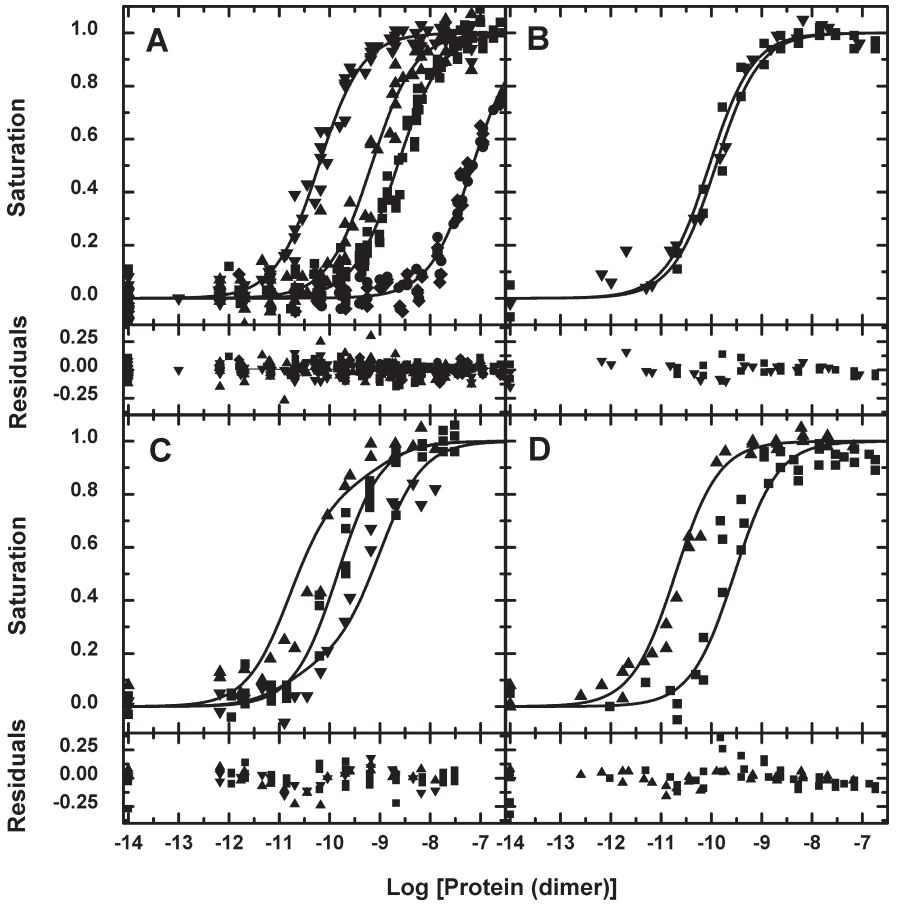

FIGURE 3: Individual site isotherms for binding of CytR and CRP(cAMP)$_1$ to *cddP*. (A) Binding of either CRP(cAMP)$_1$ alone or of CytR alone. The data shown reflect multiple experiments that include wild-type *cddP* and also reduced-valence CRP1$^-$ and CRP2$^-$ mutant promoters. (B−D) Simultaneous binding of CRP(cAMP)$_1$ and CytR. In separate experiments, the concentration of each protein is varied in the presence of a constant concentration of the other. Each panel represents a different promoter: (B) CRP1$^-$; (C) wild type; (D) CRP2$^-$. Symbols denote the different binding interactions: ▼, CRP binding to CRP1; ▲, CRP binding to CRP2; ■ CytR binding to CytO; ◆, CytR binding to the CytR site located at CRP1; ●, CytR binding to the CytR site located at CRP2. The solid curves represent the global analysis of all data according to the model defined in Table 2. Residuals from the global analysis are shown below each panel.

coupled energetics for binding of CytR and CRP to their primary operators, but without regard to any particular sequence of DNA, generates parameter values that are indistinguishable from those obtained from the protection actually observed. To validate further the importance of competition, ΔG_4 and ΔG_5 were held fixed at 0 kcal/mol. The resulting parameters do not describe the data well for CRP2 and CRP1 in the presence and absence of CytR, respectively. These observations provide strong support for the molecular model.

Based on these results, ΔG_4 and ΔG_5 were held fixed as equal to −9.6 kcal/mol to generate the parameter estimates shown in Table 4 and the curves shown in Figure 3. The values of ΔG_1, ΔG_2, and ΔG_3 are statistically indistinguishable from the $\Delta G_{\mathrm{Load},i}$ values listed in Table 1 for CytR binding alone to CytO and for CRP binding alone to both CRP1 and CRP2. ΔG_{13} and ΔG_{23}, which represent pairwise cooperative interactions between CRP and CytR at *cddP*, yielded values (−1.0 ± 0.4 kcal/mol and −1.7 ± 0.4 kcal/mol) that are very similar to what was obtained for both *deoP2* (−1.4 kcal/mol and −1.5 kcal/mol) and *udpP* (−1.4 kcal/mol and −1.3 kcal/mol) (*19*, *22*). These similarities suggest that neither operator sequence differences, spacing between CytO half-sites, nor variations in the location of CytO between CRP1 and CRP2 strongly affect the pairwise interactions between unliganded CytR and CRP. There does appear to be an effect on the way in which these pairwise interactions combine to yield the three-way cooperative interaction, ΔG_{123}. The value we obtain for *cddP* (−1.5 (+0.4, −0.3) kcal/mol; Table 4) is less cooperative than both *udpP* (−2.3 ± 0.3 kcal/mol) (*22*) and *deoP2* (−3.1 ± 0.4 kcal/mol) (*19*).

Table 4: Global Analysis of Individual Site Binding Data Represented in Table 1 according to the Model Described in Table 2

parameter	value[a]
ΔG_1	−13.6 ± 0.2
ΔG_2	−12.2 ± 0.3
ΔG_3	−11.6 ± 0.2
ΔG_{13}	−1 ± 0.4
ΔG_{23}	−1.7 ± 0.4
ΔG_{123}	−1.5 (+0.4, −0.3)
s[b]	0.054

[a]Asymmetric confidence limits are noted separately in parentheses where applicable. [b]Square root of the variance of the fitted curves.

Effect of Cytidine Binding to CytR on Cooperativity. While regulatory ligand binding to most LacI family proteins is coupled intrinsic DNA-binding affinity, in CytR, cytidine binding is coupled to protein−protein cooperativity and not to intrinsic protein−DNA-binding affinity. The lack of effect on intrinsic DNA binding was verified by control experiments at *cddP*.

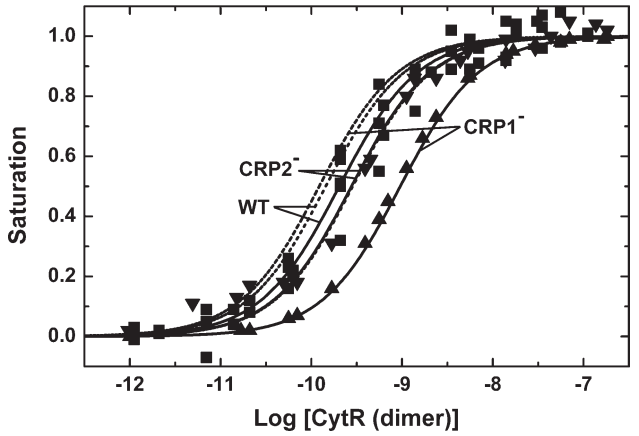

FIGURE 4: Effect of inducer cytidine on cooperative binding of CytR to *cddP*. CytR binding to CytO in wild-type (■), CRP1$^-$ (▲), and CRP2$^-$ (▼) *cddP* in the presence of saturating CRP(cAMP)$_1$ (64 nM) and cytidine (2 mM). The solid curves represent the global analysis of the binding data to the model described in Table 2 as described in the text. The dashed curves are the isotherms from Figure 3 for binding of apo-CytR to these same sites under the same conditions.

Table 5: Global Analysis of Individual Site Titration Data Including Those with Cytidine Present As Represented in Table 1 according to the Model Described in Table 3

parameter	value[a]
$\Delta\Delta G_{13}$	−0.2 (+0.2, −0.3)
$\Delta\Delta G_{23}$	+1.1 ± 0.4
$\Delta\Delta G_{123}$	+0.2 ± 0.4
s[b]	0.054

[a]Asymmetric confidence limits are noted separately in parentheses where applicable. [b]Square root of the variance of the fitted curves.

In order to analyze the effect of inducer binding to CytR on CytR-CRP cooperativity, a second set of experiments was conducted with cytidine-liganded CytR and global analysis performed as described above. Figure 4 compares results for binding of unliganded versus cytidine-liganded CytR to CRP-liganded *cddP*. Loss of cooperativity is evidenced by the rightward shift of the titration curves for cytidine-liganded CytR. A large effect is observed in the case when CRP is bound to CRP2 but not to CRP1 (reduced-valence CRP1$^-$ *cddP*), suggesting a substantial decrease in pairwise cooperativity, ΔG_{23}. In contrast, there is essentially no effect when CRP is bound to CRP1 but not to CRP2 (reduced-valence CRP2$^-$ *cddP*) and only a small effect when CRP is bound to both sites (wild-type *cddP*).

The parameter values obtained from the model-dependent global analysis are presented in Table 5. These bear out the qualitative observations from Figure 4: $\Delta\Delta G_{13}$ and $\Delta\Delta G_{123}$ values are approximately zero within the confidence intervals reported, while $\Delta\Delta G_{23}$ indicates nearly complete loss of pairwise cooperativity. This represents a third pattern of cytidine linked effects as compared to *deoP2*, for which both pairwise cooperative interactions are essentially eliminated, and *udpP*, for which pairwise cooperativity is lost for CRP1 but retained for CRP2.

DISCUSSION

The combinatorial assembly of multiple transcription factors is a primary mechanism of gene regulation in all organisms. The CytR regulon provides an ideal model to study combinatorial

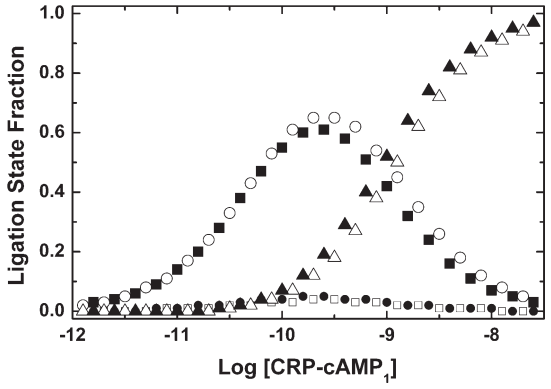

FIGURE 5: Comparison of the distributions of CRP ligation states of *cddP* and *udpP* calculated using the free energy changes for binding of CRP(cAMP)$_1$ to CRP1 and CRP2 as described in the text. The solid symbols denote *cddP* and the open symbols, *udpP*. Squares denote CRP1 filled and CRP2 empty; circles, CRP2 filled and CRP1 empty; triangles, both CRP1 and CRP2 filled. Because CRP1 and CRP2 mediate different activation mechanisms, the symbols can also be considered to indicate activation mechanisms as follows: (■, □) *cddP* and *udpP* class II, respectively; (●, ○) *cddP* and *udpP* class I, respectively; (▲, △) *cddP* and *udpP* class III, respectively. The pattern of activation of *deoP2* would be roughly similar to *udpP* and not *cddP*.

gene regulation because the number of transcription factors involved is quite small, only two, yet the extents of activation, repression, and induction vary substantially between the different promoters whose architectures are very similar. Coordinate gene regulation is achieved by nesting local repression by the LacI family member, CytR, on the global activation mediated by CRP. The interactions between these two transcription factors are modulated by the scaffolding effect of slightly different arrangements of regulatory elements. As shown in Figure 1, the locations of the CRP sites are roughly the same for all three promoters. The differences between the promoters are in regard to the location and half-site spacing of the CytR operator sites. The result of these differences in promoter architecture is wide-ranging levels of regulation at each of the class III promoters.

The molecular basis for combinatorial gene regulation is the site-specific and typically cooperative assembly of gene regulatory, protein−DNA complexes, a process that is governed by the energetics of the individual protein−DNA, protein−protein, and protein−ligand interactions. The DNase I footprint method used here provides a unique experimental signal for each local interaction. By analyzing these titration data with a quantitative model that accurately accounts for all interactions, we have been able to determine intrinsic free energy changes both for intrinsic transcription factor binding to DNA and for the cooperative and competitive interactions between the transcription factors. With this information, the distributions of ligation states of each of the promoters under physiologically relevant concentrations of CRP and CytR are easily computed. It should be possible to infer which ligation states are functionally important for activation and repression by correlating the different distributions to the different regulatory properties of the promoters.

The first important result obtained in this regard is that CRP1 is a much higher affinity site than CRP2 in *cddP*, exactly the opposite of the situation in both *deoP2* and *updP*. This of course is evident directly from the loading free energy changes compiled in Table 1, completely independent of any model-dependent analysis. The consequences of this fact on the distribution of CRP-bound states (assuming no CytR binding) are plotted as a

function of CRP-cAMP concentration in Figure 5. As glucose is systematically replaced as the primary carbon source, the intracellular cAMP concentration increases, resulting in the changing distribution of CRP-bound states from left to right in the figure. *CddP* with CRP-cAMP bound to CRP1, but not CRP2, accumulates to a high level, becoming the predominant species at intermediate cAMP concentration. CRP2 fills only at higher cAMP levels and almost entirely to promoters in which CRP1 is already filled; the 10-fold difference in intrinsic binding affinities results in only a negligible fraction of CRP2-filled, but CRP1-empty, *cddP*. Figure 5 also shows the distribution for *udpP*; though not shown, *deoP2* is similar. At these promoters, it is CRP2-filled but CRP1-empty that accumulates at intermediate cAMP concentration. The 10−20-fold affinity difference between the sites results in a negligible fraction of CRP1-filled, CRP2-empty.

The significance of this difference is easily understood in the context of the dual transcriptional activation mechanisms mediated by CRP. The class I activation mechanism that CRP utilizes when bound to CRP2 recruits RNAP via an interaction between the promoter proximal subunit of the CRP dimer and the polymerase α-CTD. The class II mechanism that CRP utilizes when bound to CRP1 also features this interaction, although in this case with the promoter distal subunit of bound CRP. But, in addition, a second surface of the promoter proximal subunit CRP interacts with the α-NTD, which activates the polymerase allosterically to increase the rate of open complex formation (*17*, *33*).

The CytR-regulated class III promoters combine both class I and class II mechanisms, presumably to confer the greatest variation in CRP-mediated activation. However, the ways in which class I and class II mechanisms of activation combine to yield such variable class III activation has not been investigated thoroughly. Our results illustrate one very simple way to generate variable class III activation, the basis of which is found in reporter gene studies using synthetic class III promoters that indicate more than an order of magnitude higher fold activation from the class II mechanism than from the class I mechanism (*34*). This would necessarily lead to a two-step activation mechanism at both *deoP2* and *udpP*: first, a relatively modest activation due to the initial recruitment of RNAP by CRP bound at CRP2. As the higher affinity of the two operators, CRP2 fills first most of the time at these two promoters. This generates a class I activation mechanism. This is followed by strong allosteric activation as CRP subsequently fills CRP1, the lower affinity of the two CRP sites at these promoters. The allosteric mechanism is class II. However, since CRP2 fills first most of the time, the result of CRP1 filling typically results in both class I and class II activation; this combination is what we refer to as class III. In addition, concomitant with CRP binding to CRP1, CytR will tend binding to CytO, due to its recruitment by the strong three-way cooperative interactions. This two-step activation mechanism is responsive to a wide range of cAMP concentrations but is also repressed well before attaining its maximum potential. Consistent with this expectation, activation is limited to only about 30× at *deoP2* and 50× at *udp* (*2*, *35*−*38*).

Activation at *cddP* is much different from this as a result of the opposite order of affinity for CRP binding to CRP1 and CRP2. At *cddP*, initial binding of CRP to is primarily to CRP1 where it will activate via a class II mechanism. Consistent with expectations that the class II mechanism yields strong activation, CRP1 alone is reported to generate ca. 225-fold activation of *cddP* whereas CRP2 alone generates much weaker activation (*2*, *3*). Consequently, the subsequent binding of CRP to CRP2 should contribute only a relatively modest increment to the overall activation, and even this would be muted to a substantial extent as a result of concomitant recruitment of CytR to CytO that results from the strong three-way cooperativity. The overall result expected is robust and essentially single-step activation as CRP1 fills, followed by repression as CRP2 and CytO both fill. Not only is the relative affinity of CRP higher for CRP1 than for CRP2, but also the absolute affinity of CRP for CRP1 is unusually high. CRP1 of *cddP* exhibits the highest affinity for CRP of any site in CytR-regulated promoters. On this basis, *cddP* would be expected to be the first CytR-regulated promoter to respond to elevated cAMP concentration and to exhibit the strongest activation. Consistent with these expectations, *cddP* exhibits the highest level of activation *in vivo*, reported to be roughly 950-fold with glycerol as a carbon source (*2*, *3*).

Another significant observation of the *cddP* footprints is the unusually high affinity for CytR binding, both to CytO (Table 4) and also to the site located just downstream from the transcription start site (Figure 2). CytO at *cdd* is the highest affinity CytR binding site investigated so far. The combination of relatively low affinity of CRP2, high affinity of CytO, and greater CytR-CRP1 and three-way than CytR-CRP1 cooperativity (Table 4) assures that CytO fills essentially concomitant with CRP2. If the unusually high affinity for CRP imparts both high sensitivity to cAMP concentration and also contributes to high levels of CRP-mediated activation, the high affinity for CytR binding to CytO counteracts this with high sensitivity repression, thus making *cddP* both the first to turn on and the first to shut off of the CytR-regulated promoters. CytR binding that occludes the transcription start site has also been found in *deoP2* but with nearly an order of magnitude lower affinity (*19*). The unusually high affinity CytR site occluding the *cdd* transcription start site presumably confers another level of repression of the very strong CRP-mediated activation. The net result is that CytR is similarly effective at reversing the robust CRP-mediated activation at *cddP* as it is at reversing the much weaker activation of other promoters.

CytR is unique among LacI/GalR family members in that binding of its regulatory ligand, cytidine, is linked not to DNA-binding affinity but instead to the cooperative interactions between CytR bound at CytO and CRP bound to CRP1 and CRP2. This loss of cooperativity is what underlies induction of transcription. Previously, we have found profoundly different effects of cytidine binding on cooperativity. At *deoP2*, cooperativity is largely eliminated (*19*). Since cooperativity contributes over 2 orders of magnitude to the effective affinity for CytR binding, the effect is simply analogous to a decrease in intrinsic DNA-binding affinity. Induction would be easily understood to be the result of decreased occupancy of CytO by CytR. At *udpP*, however, the pairwise interaction between CytR and CRP bound to CRP2 is essentially unaffected (*22*). The pairwise interaction between CytR and CRP bound to CRP1 is greatly reduced, but because CRP2 is the weaker site and as such is rarely occupied by itself, the reduction in pairwise CytR-CRP2 has a negligible effect. In addition, because the pairwise CytR-CRP2 and CytR-CRP1 cooperative interactions are not additive, the three-way CRP-CytR-CRP cooperative interaction is only modestly affected ($\Delta\Delta G_{123} = +0.8 \pm 0.4$ (*22*)). It seems fairly evident that this difference, accounting for only about a 3-fold effect on affinity, is insufficient to account for induction simply on the basis of reduced CytO occupancy.

Our *cddP* data demonstrate yet a third pattern of effects on cooperativity, in which the pairwise interaction between CytR and CRP bound to CRP1 is completely unaffected while the pairwise interaction between CytR and CRP bound to CRP1 is greatly reduced. Again, it is pairwise cooperativity with the weaker of the two CRP sites that is affected, and again, because the pairwise cooperative interactions are nonadditive, there is no discernible effect on three-way cooperativity (Table 5). The effective affinity of CytR for CytO (in the presence of CRP) is only 1.2 times higher than cytidine-liganded CytR, yet induction is fairly robust, accounting for a roughly 20-fold increase in transcription according to reporter gene assays (*21*). The conclusion that CytO occupancy alone does not account for repression seems inescapable. We propose instead that the CytR-CRP interactions themselves are critical to CytR-mediated repression. Either competition between CytR and RNAP for interaction with CRP is the main mechanism of repression, with RNAP-DNA interactions being essentially ancillary, or cytidine-liganded CytR remains bound to the DNA in a conformation which prevents CytR from acting as an allosteric antiactivator of either or both of the flanking CRP molecules. The result is that CRP may still be able to activate transcription via a class I or class II mechanism or a combination of both.

The work presented here demonstrates that there are more possibilities for transcriptional control than expected at this system. First, the pattern of synergistic activation due to CRP binding at both sites changes when CRP binds to the CRP1 site first. Second, we were surprised to find that CytR acts as a typical bacterial repressor by binding with high affinity to a region overlapping the RNAP binding site. Third, by binding to the CytR operator with high affinity, CytR acts as an antiactivator at lower CytR concentrations and recruits CRP at lower CRP concentrations.

Finally, the effect of the inducer cytidine is now known to allow for CRP1-mediated activation as at *cddP*, for CRP2-mediated activation as at *udpP*, or no activation from either CRP1 or CRP2 as at *deoP2*. The molecular mechanism that underlies these differing behaviors is clearly a significant issue. Although the data presented herein do not address this, some speculation is possible. The differences in behavior must reflect differences in either promoter architecture or sequence, with the former seeming more likely. Referring to Figure 1, one substantial difference in promoter architecture is that the number of base pairs that separate the inverted repeats in CytO varies quite dramatically from zero base pairs in *deoP2* to nine in *nupG*. Previously, we have shown that this spacing affects the CytR binding mode, i.e., generating what we interpret to be a rigid conformation bound to CytO at *deoP2* to a dynamically flexible conformation bound to CytO at *nupG* (*25*, *39*). We speculate that these different conformational modes restrict interactions between bound DNA-bound CytR and DNA-bound CRP in ways that are reflected in the different effects of cytidine binding to CytR in CytR-CRP cooperativity. Evaluating this hypothesis is the subject of our continuing investigations.

ACKNOWLEDGMENT

We thank Dr. Vira Tretyachenko-Ladokhina for the CytR and CRP used in this work as well as for discussion and insights. We also thank Ms. Meenakshi Rajan for cloning the *cdd* promoter DNA.

REFERENCES

1. Keseler, I. M., Bonavides-Martinez, C., Collado-Vides, J., Gama-Castro, S., Gunsalus, R. P., Johnson, D. A., Krummenacker, M., Nolan, L. M., Paley, S., Paulsen, I. T., Peralta-Gil, M., Santos-Zavaleta, A., Shearer, A. G., and Karp, P. D. (2009) EcoCyc: a comprehensive view of *Escherichia coli* biology. *Nucleic Acids Res. 37*, D464–D470.
2. Kristensen, H. H., Valentin-Hansen, P., and Sogaard-Andersen, L. (1997) Design of CytR regulated, cAMP-CRP dependent class II promoters in *Escherichia coli*: RNA polymerase-promoter interactions modulate the efficiency of CytR repression. *J. Mol. Biol. 266*, 866–876.
3. Valentin-Hansen, P., Holst, B., Josephsen, J., Hammer, K., and Albrechtsen, B. (1989) CRP/cAMP- and CytR-regulated promoters in *Escherichia coli* K12: the cdd promoter. *Mol. Microbiol. 3*, 1385–1390.
4. Sogaard-Andersen, L., and Valentin-Hansen, P. (1993) Protein-protein interactions in gene regulation: the cAMP-CRP complex sets the specificity of a second DNA-binding protein, the CytR repressor. *Cell 75*, 557–566.
5. Valentin-Hansen, P., Albrechtsen, B., and Love Larsen, J. E. (1986) DNA-protein recognition: demonstration of three genetically separated operator elements that are required for repression of the *Escherichia coli* deoCABD promoters by the DeoR repressor. *EMBO J. 5*, 2015–2021.
6. Holst, B., Sogaard, A. L., Pedersen, H., and Valentin, H. P. (1992) The cAMP-CRP/CytR nucleoprotein complex in *Escherichia coli*: two pairs of closely linked binding sites for the cAMP-CRP activator complex are involved in combinatorial regulation of the cdd promoter. *EMBO J. 11*, 3635–3643.
7. Swint-Kruse, L., and Matthews, K. S. (2009) Allostery in the LacI/GalR family: variations on a theme. *Curr. Opin. Microbiol. 12*, 129–137.
8. Tungtur, S., Egan, S. M., and Swint-Kruse, L. (2007) Functional consequences of exchanging domains between LacI and PurR are mediated by the intervening linker sequence. *Proteins: Struct., Funct., Bioinf. 68*, 375–388.
9. Martinez-Antonio, A., and Collado-Vides, J. (2003) Identifying global regulators in transcriptional regulatory networks in bacteria. *Curr. Opin. Microbiol. 6*, 482–489.
10. Kolb, A., Busby, S., Buc, H., Garges, S., and Adhya, S. (1993) Transcriptional regulation by cAMP and Its receptor protein. *Annu. Rev. Biochem. 62*, 749–795.
11. Attey, A., Belyaeva, T., Savery, N., Hoggett, J., Fujita, N., Ishihama, A., and Busby, S. (1994) Interactions between the cyclic-AMP receptor protein and the alpha-subunit of RNA-polymerase at the *Escherichia coli* galactose operon P1 promoter. *Nucleic Acids Res. 22*, 4375–4380.
12. Beatty, C. M., Browning, D. F., Busby, S. J. W., and Wolfe, A. J. (2003) Cyclic AMP receptor protein-dependent activation of the *Escherichia coli* acsP2 promoter by a synergistic class III mechanism. *J. Bacteriol. 185*, 5148–5157.
13. Belyaeva, T. A., Rhodius, V. A., Webster, C. L., and Busby, S. J. W. (1998) Transcription activation at promoters carrying tandem DNA sites for the *Escherichia coli* cyclic AMP receptor protein: organisation of the RNA polymerase alpha subunits. *J. Mol. Biol. 277*, 789–804.
14. Busby, S., and Ebright, R. H. (1997) Transcription activation at class II CAP-dependent promoters. *Mol. Microbiol. 23*, 853–859.
15. Meibom, K. L., Sogaard-Andersen, L., Mironov, A. S., and Valentin-Hansen, P. (1999) Dissection of a surface-exposed portion of the cAMP-CRP complex that mediates transcription activation and repression. *Mol. Microbiol. 32*, 497–504.
16. Wade, J. T., Belyaeva, T. A., Hyde, E. I., and Busby, S. J. W. (2001) A simple mechanism for co-dependence on two activators at an *Escherichia coli* promoter. *EMBO J. 20*, 7160–7167.
17. Rhodius, V. A., West, D. M., Webster, C. L., Busby, S. J. W., and Savery, N. J. (1997) Transcription activation at class II CRP-dependent promoters: the role of different activating regions. *Nucleic Acids Res. 25*, 326–332.
18. Pedersen, H., Sogaard, A. L., Holst, B., and Valentin-Hansen, P. (1991) Heterologous cooperativity in *Escherichia coli*. The CytR repressor both contacts DNA and the cAMP receptor protein when binding to the *deoP2* promoter. *J. Biol. Chem. 266*, 17804–17808.
19. Perini, L. T., Doherty, E. A., Werner, E., and Senear, D. F. (1996) Multiple specific CytR binding sites at the *Escherichia coli deoP2* promoter mediate both cooperative and competitive interactions between CytR and cAMP receptor protein. *J. Biol. Chem. 271*, 33242–33255.

20. Chahla, M., Wooll, J., Laue, T. M., Nguyen, N., and Senear, D. F. (2003) Role of protein-protein bridging interactions on cooperative assembly of DNA-bound CRP-CytR-CRP complex and regulation of the *Escherichia coli* CytR regulon. *Biochemistry 42*, 3812–3825.
21. Barbier, C. S., Short, S. A., and Senear, D. F. (1997) Allosteric mechanism of induction of CytR-regulated gene expression. CytR repressor-cytidine interaction. *J. Biol. Chem. 272*, 16962–16971.
22. Gavigan, S. A., Nguyen, T., Nguyen, N., and Senear, D. F. (1999) Role of multiple CytR binding sites on cooperativity, competition, and induction at the *Escherichia coli* udp promoter. *J. Biol. Chem. 274*, 16010–16019.
23. Senear, D. F., Perini, L. T., and Gavigan, S. A. (1998) Analysis of interactions between CytR and CRP at CytR-regulated promoters. *Methods Enzymol. 295*, 403–424.
24. Gronenborn, A. M., and Clore, G. M. (1986) Overproduction of the cyclic-AMP receptor protein of *Escherichia coli* and expression of the engineered C-terminal DNA-binding domain. *Biochem. J. 236*, 643–649.
25. Tretyachenko-Ladokhina, V., Ross, J. B., and Senear, D. F. (2002) Thermodynamics of *E. coli* cytidine repressor interactions with DNA: distinct modes of binding to different operators suggests a role in differential gene regulation. *J. Mol. Biol. 316*, 531–546.
26. Brenowitz, M., Senear, D. F., and Ackers, G. K. (1989) Flanking DNA-sequences contribute to the specific binding of cI-repressor and O_R1. *Nucleic Acids Res. 17*, 3747–3755.
27. Das, R., Laederach, A., Pearlman, S. M., Herschlag, D., and Altman, R. B. (2005) SAFA: semi-automated footprinting analysis software for high-throughput quantification of nucleic acid footprinting experiments. *RNA 11*, 344–354.
28. Brenowitz, M., and Senear, D. F. (1989) DNase I footprint analysis of site-specific protein-DNA binding, in Current Protocols in Molecular Biology (Ausubel, F. M., Brent, R., Kingston, R. E., Moore, D. D., Seidman, J. G., Smith, J. A., and Struhl, K., Eds.) p Unit 12.14, Greene Publishing and Wiley-Interscience, New York.
29. Senear, D. F., and Batey, R. (1991) Comparison of operator specific and nonspecific DNA binding of the lambda cI repressor; [KCl] and pH effects. *Biochemistry 30*, 6677–6688.
30. Brenowitz, M., Senear, D. F., Shea, M. A., and Ackers, G. K. (1986) Quantitative DNase footprint titration: a method for studying protein-DNA interactions. *Methods Enzymol. 130*, 132–181.
31. Ackers, G. K., Shea, M. A., and Smith, F. R. (1983) Free energy coupling within macromolecules. The chemical work of ligand binding at the individual sites in cooperative systems. *J. Mol. Biol. 170*, 223–242.
32. Senear, D. F., and Bolen, D. W. (1992) Simultaneous analysis for testing of models and parameter estimation. *Methods Enzymol. 210*, 463–481.
33. Niu, W., Kim, Y., Tau, G., Heyduk, T., and Ebright, R. H. (1996) Transcription activation at class II CAP-dependent promoters: two interactions between CAP and RNA polymerase. *Cell 87*, 1123–1134.
34. Busby, S., and Ebright, R. H. (1994) Promoter structure, promoter recognition, and transcription activation in prokaryotes. *Cell 79*, 743–746.
35. Rasmussen, P. B., Sogaard, A. L., and Valentin, H. P. (1993) Identification of the nucleotide sequence recognized by the cAMP-CRP dependent CytR repressor protein in the *deoP2* promoter in *E. coli*. *Nucleic Acids Res. 21*, 879–885.
36. Sogaard-Andersen, L., Mironov, A. S., Pedersen, H., Sukhodelets, V. V., and Valentin-Hansen, P. (1991) Single amino acid substitutions in the cAMP receptor protein specifically abolish regulation by the CytR repressor in *Escherichia coli*. *Proc. Natl. Acad. Sci. U.S.A. 88*, 4921–4925.
37. Sogaard-Andersen, L., Mollegaard, N. E., Douthwaite, S. R., and Valentin-Hansen, P. (1990) Tandem DNA-bound cAMP-CRP complexes are required for transcriptional repression of the *deoP2* promoter by the CytR repressor in *Escherichia coli*. *Mol. Microbiol. 4*, 1595–1601.
38. Valentin-Hansen, P., Holst, B., Sogaard, A. L., Martinussen, J., Nesvera, J., and Douthwaite, S. R. (1991) Design of cAMP-CRP-activated promoters in *Escherichia coli*. *Mol. Microbiol. 5*, 433–437.
39. Tretyachenko-Ladokhina, V., Cocco, M. J., and Senear, D. F. (2006) Flexibility and adaptability in binding of *E. coli* cytidine repressor to different operators suggests a role in differential gene regulation. *J. Mol. Biol. 362*, 271–286.